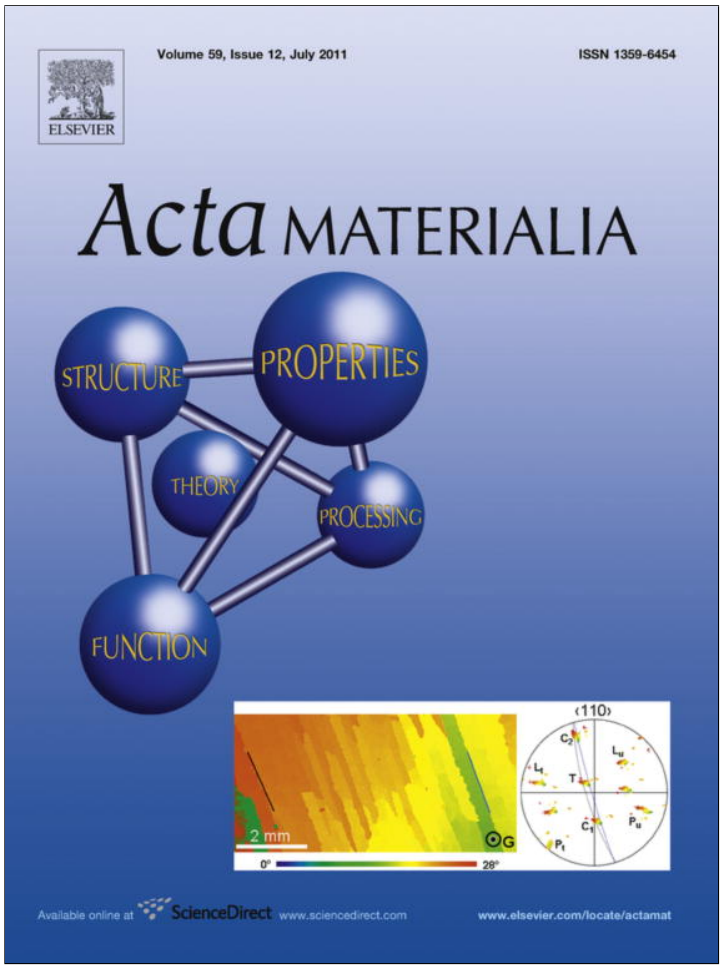

Available online at www.sciencedirect.com
ScienceDirect
Acta Materialia 59 (2011) 5023–5031
Acta MATERIALIA
www.elsevier.com/locate/actamat

# Effect of cooperative grain boundary sliding and migration on crack growth in nanocrystalline solids

I.A. Ovid'ko [a,b,*], A.G. Sheinerman [a], E.C. Aifantis [c]

[a] Institute of Problems of Mechanical Engineering, Russian Academy of Sciences, Bolshoj 61, Vasil. Ostrov, St. Petersburg 199178, Russia
[b] Department of Mathematics and Mechanics, St. Petersburg State University, St. Petersburg 198504, Russia
[c] Aristotle University of Thessaloniki, 54124 Thessaloniki, Greece

Received 3 February 2011; received in revised form 22 April 2011; accepted 25 April 2011
Available online 26 May 2011

**Abstract**

A new mechanism of fracture toughness enhancement in nanocrystalline metals and ceramics is suggested. The mechanism represents the cooperative grain boundary (GB) sliding and stress-driven GB migration process near the tips of growing cracks. It is shown that this mechanism can increase the critical stress intensity factor for crack growth in nanocrystalline materials by a factor of three or more and thus considerably enhances the fracture toughness of such materials.


*Keywords:* Nanocrystalline materials; Cracks; Grain boundary sliding; Grain boundary migration

## 1. Introduction

Nanocrystalline metals and ceramics exhibit superior mechanical properties that have attracted a rapidly growing research interest in recent years (see, e.g., original papers [1–15] and reviews [16–23]). However, in spite of their excellent mechanical characteristics (in particular, very high strength and hardness), nanocrystalline solids often demonstrate a brittle behavior, which severely limits their practical applications (see, e.g., reviews [16–23] and book [24]).

At the same time, in some cases, nanocrystalline materials exhibit considerable tensile ductility at room temperature [25–27] or superplasticity at elevated temperatures [28] as well as significant fracture toughness that can be often higher than that of their polycrystalline or single-crystalline counterparts [24,29–33]. Although the nature of good ductility and toughness of some high-strength nanocrystalline materials is not yet quite clear, it can be associated with specific deformation mechanisms, such as Coble creep [34], grain rotation and sliding [35–37] that operate in nanocrystalline solids. In particular, recently, several specific deformation mechanisms have been assumed to be responsible for the toughness enhancement in nanocrystalline solids. These include Ashby–Verall creep (carried by intergrain sliding accommodated by grain boundary (GB) diffusion and grain rotations) [7], nanoscale deformation twinning [38], rotational deformation [39] and stress-driven migration of GBs [40].

Recently, rapidly growing attention has been paid to the stress-driven migration of GBs in nanocrystalline materials, which represents both a toughening micromechanism [40] and a specific deformation mode [19,38,41–46]. This twofold role of the stress-driven migration of GBs is indirectly supported by experimental observations [47,48] of the athermal grain growth in the vicinities of cracks in nanocrystalline materials.

Another important deformation mechanism in nanocrystalline materials is GB sliding (see, e.g., Refs. [17–20,24]). Non-accommodated GB sliding in nanocrystalline solids

* Corresponding author at: Institute of Problems of Mechanical Engineering, Russian Academy of Sciences, Bolshoj 61, Vasil. Ostrov, St. Petersburg 199178, Russia. Tel.: +7 812 321 4764; fax: +7 812 321 4771.
*E-mail address:* ovidko@nano.ipme.ru (I.A. Ovid'ko).

1359-6454/$36.00 
doi:10.1016/j.actamat.2011.04.056

creates defects (dislocations and disclination dipoles) at triple junctions of GBs, which can initiate the formation of cracks, resulting in brittle fracture of nanocrystalline solids [49,50]. At the same time, if GB sliding is effectively accommodated, nanocrystalline solids show enhanced ductility and/or superplasticity [24,28,51]. Accommodation of GB sliding can be effectively realized through lattice dislocation emission from triple junctions or diffusion [24,28,51]. Recently, a new way to accommodate GB sliding through GB migration has been suggested and theoretically analyzed [52]. The discussed (new) accommodation mode results in the deformation mechanism that involves the cooperative GB sliding and stress-driven GB migration. In this case, defects created by GB sliding are, in part, accommodated by defects created by GB migration. As a corollary, cooperative GB sliding and migration serves as a special deformation mode enhanced compared to pure GB sliding in nanocrystalline materials [52]. This view is supported by numerous experimental observations [19,28,51,53] of concurrent GB sliding and grain growth occurring in nanocrystalline solids during (super)plastic deformation. In Ref. [52], cooperative GB sliding and migration was theoretically described as a deformation mode operating in crack-free nanocrystalline materials. The main aims of this paper are (i) to describe operation of the cooperative GB sliding and migration process near crack tips; and (ii) to theoretically analyze its effect (associated with the local stress relaxation near crack tips) on the fracture toughness of nanocrystalline materials.

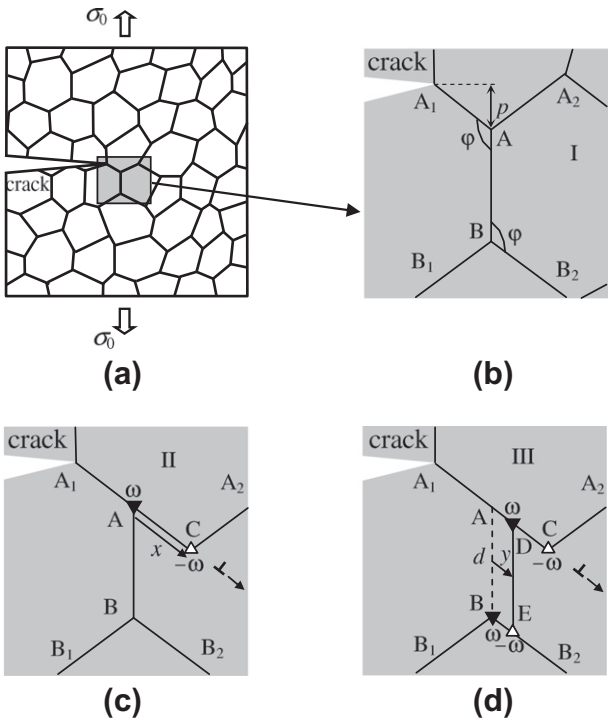


Fig. 1. Grain boundary deformation processes in nanocrystalline specimen near a crack tip. (a) General view. (b) Initial configuration I of grain boundaries. (c) Configuration II results from pure grain boundary sliding. Dipole of disclinations AC is generated due to grain boundary sliding. (d) Configuration III results from cooperative grain boundary sliding and migration process. Two disclination dipoles CD and BE are generated due to this cooperative process.

## 2. Cooperative grain boundary migration and sliding near a crack tip: model

Let us consider the geometric features of cooperative GB sliding and migration in a deformed nanocrystalline specimen with a crack (Fig. 1). For definiteness, we focus our analysis on the situation where the crack is flat, and the specimen is under a tensile load $\sigma_0$ normal to the crack plane; that is, a mode I cracking (Fig. 1a). In general, one can distinguish the following geometric types of cracks in nanocrystalline materials: intragrain cracks (propagating mostly inside grains; Fig. 1a) and intergrain or GB cracks (propagating mostly along GBs; Fig. 2a). The intergranular fracture (Fig. 2a) tends to dominate in nanocrystalline materials with finest grains (see, e.g., Refs. [24,54–56]. In doing so, crack surfaces are curved with the characteristic size of "curvature facets" being close to the grain size (Fig. 2a). Since the grain size is very low in nanocrystalline materials with finest grains, the characteristic size of "curvature facets" is commonly much lower than the crack length (Fig. 2a). As a corollary, in the situations where the role of cracks as stress sources is of critical importance, intergrain cracks in nanocrystalline materials with finest grains are effectively modeled as flat cracks (Fig. 2). The role of cracks as stress sources is dominant in initiation of the cooperative GB sliding and migration process as well as its effect on the stress relaxation near crack tips. Therefore, we will use the discussed approximation (Fig. 2) in our further analysis of the process and its effects on the local stress relaxation.

Generally speaking, the approximation illustrated in Fig. 2 can also be exploited in analysis of the tendency of a material to exhibit either intergranular or intragranular fracture behavior. In this case, however, its correctness is not self-evident from geometry, and it can be used only as a first approximation. With the approximation illustrated

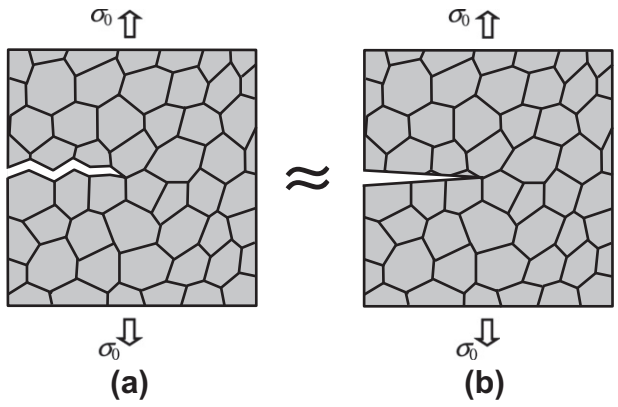


Fig. 2. A nanoscopically curved intergrain crack and its flat model. (a) A curved intergrain crack in a nanocrystalline specimen is modeled as (b) a flat crack.

in Fig. 2, the difference in crack growth conditions between intragrain cracks (Fig. 1a) and intergrain cracks (Fig. 2a) is only in the value of the surface energy penalty due to formation of crack surfaces. Growth of cracks in grain interiors (Fig. 1a) is specified by the surface energy penalty $\gamma_e = \gamma$ with $\gamma$ being the specific surface energy. Growth of intergrain cracks (Fig. 2a) is specified by the surface energy penalty $\gamma_e = \gamma - \gamma_b/2$, where $\gamma_b$ is the specific GB energy (released when the crack moves along the GB).

According to our estimates based on the approximation illustrated in Fig. 2 (see Appendix A), growth of GB cracks in nanocrystalline materials with finest grains is more preferred than growth of intragrain cracks. This theoretical statement is in good agreement with the experimentally documented trend (see, e.g., Refs. [24,54–56]) that intergranular fracture is dominant in nanocrystalline materials with finest grains. The agreement in question indirectly supports use of the approximation (Fig. 2) in our further examination of the cooperative GB sliding and migration process as well as its effect on the stress relaxation near the crack tip in nanocrystalline materials with finest grains.

Thus, let us consider a nanocrystalline specimen which contains a flat crack and is under a tensile load $\sigma_0$ normal to the crack plane (Fig. 1a). The applied load and high stress concentration near the crack tip can induce both GB migration and sliding near this tip (Fig. 1). These processes release, in part, the high elastic stresses near the crack tip and thereby can slow down crack growth. Assuming that the intensity of GB migration and sliding and their effect on crack growth strongly increase with a decrease of the distance between the crack tip and GBs involved in these processes, it is reasonable to believe that the dominant effect of GB migration and sliding processes on crack propagation may be determined by these processes near the tip.

In the following, we will focus our consideration on the case of cooperative GB sliding and migration in the vicinity of crack tips. The geometry of this deformation mechanism is schematically presented in Fig. 1. Fig. 1a depicts a two-dimensional (2-D) section of a deformed nanocrystalline specimen. Within the model [52], GB sliding occurs under the applied shear stress and transforms the initial configuration I of GBs (Fig. 1b) into configuration II (Fig. 1c). GB sliding is assumed to be accommodated, in part, by emission of lattice dislocations from triple junctions (Fig. 1c). Besides, following Refs. [49,50], GB sliding results in the formation of a dipole of wedge disclinations A and C in configuration II (Fig. 1c) characterized by strengths $\pm\omega$, whose magnitude $\omega$ is equal to the tilt misorientation of the GB (AB is assumed to be a symmetric tilt boundary). The disclination dipole AC has an arm (the distance between the disclinations) equal to the magnitude $x$ of the relative displacement of grains (Fig. 1c).

We further assume [52] that, in parallel with GB sliding, stress-driven GB migration occurs as well, so that the stress fields of defects created by GB sliding are, in part, accommodated by the defects created by GB migration. In the case shown in Fig. 1, the migration of the grain boundary AB into another position DE results in the formation of a quadrupole of wedge disclinations with the strengths $\pm\omega$ at the points A, B, D and E [52]. The disclination with the strength $+\omega$ appearing at the point A due to GB sliding and the disclination with the strength $-\omega$ appearing at the same point due to GB migration annihilate. The annihilation results in the disclination configuration shown in Fig. 1d. In general, the cooperative GB sliding and migration process transforms the initial configuration I (Fig. 1b) into the final configuration III (Fig. 1d). During this processes, in parallel with GB sliding that causes the relative displacement of grains over the distance $x$, stress-driven migration of the vertical GB occurs over the distance $y$ from its initial position AB to the new position DE (Fig. 1d). The cooperative GB sliding and migration process leads to the formation of two disclination dipoles CD and BE (Fig. 1d). The disclination dipole CD of wedge disclinations is characterized by the strength magnitude $\omega$ and the arm $|x - y|$. The disclination dipole BE is characterized by the strength magnitude $\omega$ and the arm $y$.

## 3. Energy characteristics of cooperative grain boundary migration and sliding process: its effects on critical stress intensity factor for crack growth in nanocrystalline solids

Let us now consider the effect of the applied tensile load and a long flat mode I crack on the cooperative GB sliding and migration process in a nanocrystalline specimen (Fig. 1). The specimen is supposed to be an elastically isotropic solid characterized by the shear modulus $G$ and Poisson's ratio $\nu$. The vertical GB is assumed to be normal to the crack growth direction and make an angle $\varphi$ with the grain boundaries $AA_1$ and $BB_2$ (Fig. 1b). Let the triple junction A lie at a distance $p$ from the crack tip and the length of all GBs in the initial state (Fig. 1b) be denoted as $d$. To calculate the parameters of the cooperative GB sliding and migration process, let us first calculate the energy change $\Delta W$ associated with the formation of the disclination configuration shown in Fig. 1d. The energy change $\Delta W$ can be written as

$$\Delta W = \sum_{j=1}^{4} W^{\Delta}(r_j, \theta_j) + \sum_{j=1}^{4} s_j W^{\Delta-\sigma}(r_j, \theta_j) + \sum_{j=1}^{4} \sum_{k=1}^{j-1} s_j s_k W_{\mathrm{int}}(r_j, r_k, \theta_j, \theta_k) - A_{sl} \quad (1)$$

where $(r_j, \theta_j)$ are the coordinates of the $j$th disclination in the polar coordinate system with the origin at the crack tip ($j = 1$–4; see Fig. 1), and the rest of the symbols are defined as follows: $W^{\Delta}(r_j, \theta_j)$ is the energy of the $j$th disclination in the solid with a crack; $W^{\Delta-\sigma}(r_j, \theta_j)$ is the energy of the interaction between the disclination with the strength $+\omega$, lying in the point $(r_j, \theta_j)$, and the stress field $\sigma_{il}$ induced by the applied load near the crack tip; $W_{\mathrm{int}}(r_j, r_k, \theta_j, \theta_k)$ is the energy of the interaction between the $j$th and $k$th disclinations

(in the solid with a crack) assuming that both disclinations have the strength $+\omega$, and $A_{sl}$ is the work of the stress $\sigma_{il}$ done on GB sliding, which does not account the formation of disclinations. The parameters $s_j$ in Eq. (1) account for the sign of a specified disclination and are defined as $s_1 = s_4 = 1$, $s_2 = s_3 = -1$. The coordinates $(r_j, \theta_j)$ are calculated as follows:

$$r_1(y) = (y^2 + p^2 - 2yp\cos\varphi)^{1/2},$$
$$r_2(x) = (x^2 + p^2 - 2xp\cos\varphi)^{1/2},$$
$$r_3(y) = (y^2 + (p+d)^2 - 2y(p+d)\cos\varphi)^{1/2},$$
$$r_4 = p + d$$
$$\theta_1(y) = -\arccos(y\sin\varphi/r_1),$$
$$\theta_2(x) = -\arccos(x\sin\varphi/r_2),$$
$$\theta_3(y) = -\arccos(y\sin\varphi/r_3),$$
$$\theta_4 = -\pi/2$$

In Eq. (1), we neglected the resistance to GB sliding associated with both the "friction" of the grain boundary $AA_1$ and the increase of its length in the course of GB sliding.

The energy term $W^{\Delta}(r,\theta)$ can be written as $W^{\Delta}(r,\theta) = \frac{G\omega^2 d^2 h(r/d)}{4\pi(1-\nu)}$, where $h(r/d)$ is a known function [39]. Similarly, the energy term $W_{\rm int}(r_j, r_k, \theta_j, \theta_k)$ can be written as follows:

$$W_{\rm int}(r_j, r_k, \theta_j, \theta_k) = \frac{G\omega^2 d^2 g(r_j/d, r_k/d, \theta_j, \theta_k)}{4\pi(1-\nu)}$$

where $g(r_j/d, r_k/d, \theta_j, \theta_k)$ is also a known function [39]. The energy term $W^{\Delta-\sigma}(r,\theta)$ follows from the expression [57]

$$W^{\Delta-\sigma}(r,\theta) = \omega\int_0^r \sigma_{\theta\theta}(r',\theta)(r-r')dr' \quad (2)$$

The component $\sigma_{\theta\theta}(r,\theta)$ of the stress field $\sigma_{il}(r,\theta)$ is given [58] by

$$\sigma_{\theta\theta}(r,\theta) = \frac{K_I^{\sigma}\cos^3(\theta/2)}{\sqrt{2\pi r}} \quad (3)$$

where $K_I$ is the stress intensity factor associated with the applied load $\sigma_0$. Substitution of Eq. (3) into Eq. (2) yields

$$W^{\Delta-\sigma}(r,\theta) = \frac{4\omega K_I^{\sigma} r^{3/2}\cos^3(\theta/2)}{3\sqrt{2\pi}} \quad (4)$$

The work $A_{sl}$ of the stress $\sigma_{il}$ done on GB sliding is calculated as the work of the stress $\sigma_{il}$ necessary to transfer a dislocation with the Burgers vector magnitude $x$ (equal to the length of GB sliding) across a grain boundary $AA_1$ of length $d$, i.e.

$$A_{sl} = x\int_0^d \sigma_{x'y'}(x')dx' \quad (5)$$

where $(x', y')$ is the Cartesian coordinate system with the origin at the crack tip and the $x'$-axis parallel to the grain boundary AA′ (Fig. 1), and the component $\sigma_{x'y'}(r,\theta)$ of the stress field $\sigma_{il}(r,\theta)$ follows from Ref. [58] as

$$\sigma_{x'y'}(x') = -\frac{K_I^{\sigma}\sin\theta_2(x')\cos^2(3\theta_2(x')/2 + 2\varphi)}{2\sqrt{2\pi r_2(x')}} \quad (6)$$

With Eq. (6) inserted into Eq. (5), we find:

$$A_{sl} = -\frac{xK_I^{\sigma}}{2\sqrt{2\pi}}\int_0^d \frac{\sin\theta_2(x')\cos^2(3\theta_2(x')/2 + 2\varphi)}{\sqrt{r_2(x')}}dx' \quad (7)$$

Thus, we have obtained appropriate expressions for all the energy terms appearing in Eq. (1) for the total energy $\Delta W$. The contour maps $\Delta W(x/d, y/d)$ are shown in Fig. 3, for the situation with nanocrystalline Ni and $K_I^{\sigma} = K_{IC}^{br}$, where $K_{IC}^{br} = \sqrt{4G\gamma_e/(1-\nu)}$ is the critical value of the stress intensity factor in the absence of disclinations (that is, in the case of brittle fracture). In general, $K_{IC}^{br}$ depends on $\gamma_e$, where $\gamma_e = \gamma$ in the case of an intragrain crack, and $\gamma_e = \gamma - \gamma_b/2$ in the case of a GB crack, with $\gamma$ and $\gamma_b$ being the specific surface energy and specific GB energy, respectively. Fig. 3 presents the contour maps $\Delta W(x/d, y/d)$, for intragrain cracks. In plotting Fig. 3, we used the following typical values of parameters of

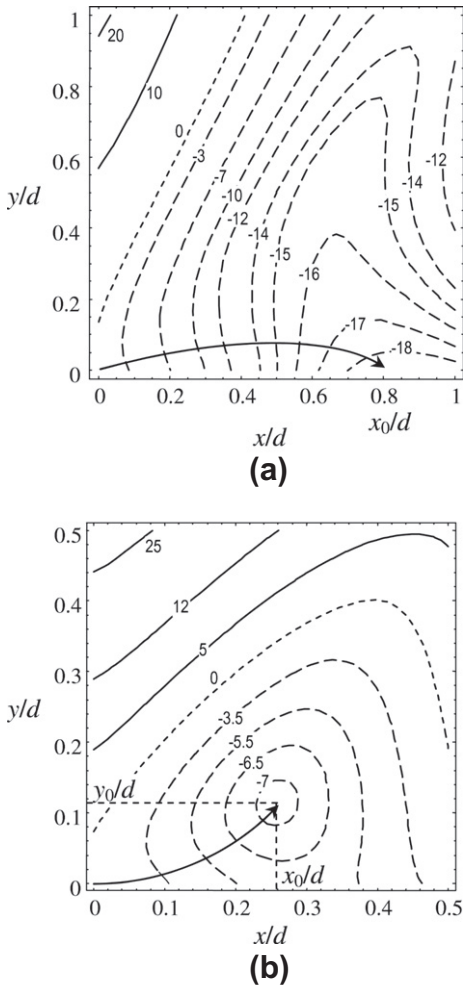


Fig. 3. Contour maps of the energy change $\Delta W$ associated with the cooperative grain boundary migration and sliding process (near the tip of a large mode I crack in nanocrystalline Ni) in the coordinate space $(x/d, y/d)$, for the case $\omega = 17°$ (a) and 30° (b). The energy $\Delta W$ is given in units of $10^{-8}$ J m$^{-1}$.

nanocrystalline Ni and its structure: $G = 73$ GPa [59], $\nu = 0.31$ [59], $\gamma = 1.725$ J m$^{-2}$ [60], $\varphi = 2\pi/3$, $d = 15$ nm, $p = 0$, $\omega = 17°$ (Fig. 3a) and 30° (Fig. 3b). The curves with arrows in Fig. 3 show the lines of the largest (in magnitude) energy gradient. As it follows from Fig. 3, if the disclination strength $\omega$ is not very large (Fig. 3a), the minimum of $\Delta W(x/d, y/d)$ corresponds to some equilibrium value $x = x_0$ of the GB sliding length, while the equilibrium value of the GB migration length $y$ is equal to zero. That is, in the discussed equilibrium state, GB migration is absent. At the same time, for large enough values of $\omega$ (Fig. 3b), the minimum of $\Delta W(x/d, y/d)$ corresponds to some equilibrium values $x = x_0$ and $y = y_0$ of the lengths of GB sliding and GB migration, respectively.

According to Fig. 3a, for small values of $\omega$, one can suggest the following scenario of the cooperative GB migration and sliding process (with the logical assumption that the lengths $x$ and $y$ change making the gradient of the energy $\Delta W$ maximum in magnitude). At the first stage of the process, both the characteristic lengths $x$ and $y$ increase; that is, GB sliding is accompanied by GB migration. However, when the length $x$ of GB sliding exceeds some critical value (equal to approximately $d/2$ in the case shown in Fig. 3a), the length $y$ of GB migration decreases; that is, GB migration changes its direction. Eventually, when the length of GB sliding reaches its equilibrium value $x = x_0$, the migrating GB returns to its original position, and thus $y = 0$. Apparently, such a behavior is associated with a complicated interplay of the disclinations (that result from GB sliding and GB migration) with each other as well as with the stress field induced by the applied load near the crack tip.

The dependences of the parameters $x_0/d$ and $y_0/d$ on the disclination strength $\omega$ are presented in Fig. 4, for the parameter values specified above. As is seen in Fig. 4, the equilibrium length of GB migration is small compared to the length of GB sliding at the considered values of the stress intensity factor $K_I^\sigma$. At the same time, according to our numerical analysis in the situation with higher values of $K_I^\sigma$, the difference between the normalized equilibrium lengths $x_0/d$ and $y_0/d$ diminishes, so that the contribution of GB migration (if such migration occurs) to the hindering of crack propagation increases. For large enough values of

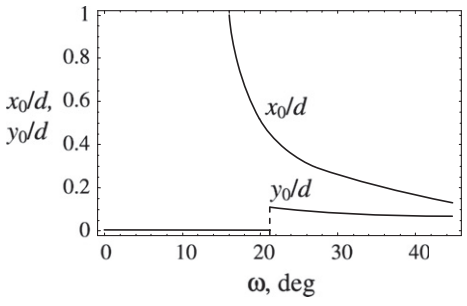


Fig. 4. Dependences of the normalized equilibrium lengths, $x_0/d$ and $y_0/d$, of grain boundary sliding and migration, respectively (near a crack tip in nanocrystalline Ni) on disclination strength $\omega$.

$\omega$, the equilibrium lengths $x_0$ and $y_0$ gradually increase with decreasing $\omega$. Below a critical value of $\omega$ ($\omega \approx 21°$), the equilibrium length $y_0$ of GB migration becomes equal to zero, whereas the equilibrium length of GB sliding $x_0$ increases very rapidly with a decrease in $\omega$, reaching the values close to the GB length $d$.

Now let us consider the effect of disclination configuration, resulting from the cooperative GB migration and sliding, on the fracture toughness of a nanocrystalline solid. To do so, we will use the standard crack growth criterion [61] based on the balance between the driving force related to a decrease in the elastic energy and the hampering force related to occurrence of a new free surface during crack growth. In the examined case of the plane strain state, this criterion is given [61] by

$$\frac{1-\nu}{2G}(K_I^2 + K_{II}^2) = 2\gamma \tag{8}$$

where $K_I$ (mode I) and $K_{II}$ (mode II) are the stress intensity factors for normal (to crack plane) and shear loading, respectively. In the considered situation where the crack growth direction is perpendicular to the direction of the external load, the coefficients $K_I$ and $K_{II}$ are given by the expressions

$$K_I = K_I^\sigma + k_I^q, \quad K_{II} = k_{II}^q \tag{9}$$

where $k_I^q$ and $k_{II}^q$ are the stress intensity factors associated with the internal stresses created by the disclinations located near the crack tip (Fig. 1).

Within the above macroscopic mechanical description, the effect of the local plastic flow – the cooperative GB migration and sliding mechanism resulting in the formation of wedge disclinations – on crack growth can be accounted for through the introduction of the critical stress intensity factor $K_{IC}$. In this case, the crack is considered as that propagating under the action of the tensile load perpendicular to the crack growth direction, while the presence of the disclinations simply changes the value of $K_{IC}$ corresponding to the case of brittle crack propagation. In these circumstances, the critical condition for the crack growth can be represented as (e.g., Ref. [58]): $K_I^\sigma = K_{IC}$.

With substitution of Eq. (9) into Eq. (8) and use of the critical condition $K_I^\sigma = K_{IC}$, one finds the following expression for $K_{IC}$ [39]:

$$K_{IC} = \sqrt{(K_{IC}^{br})^2 - (k_{IIC}^q)^2} - k_{IC}^q \tag{10}$$

The quantities in Eq. (10) are defined as follows: $K_{IC}^{br} = \sqrt{4G\gamma/(1-\nu)}$, as above, $k_{IIC}^q = k_{II}^q|_{K_I^\sigma = K_{IC}}$, and $k_{IC}^q = k_I^q|_{K_I^\sigma = K_{IC}}$. It should be noted that the quantities $k_{IIC}^q$ and $k_{IC}^q$ depend on $K_{IC}$, and, thus, Eq. (10) provides the appropriate formula for the determination of $K_{IC}$.

The quantities $k_I^q$ and $k_{II}^q$ appearing in the above expression are given [39] by the following relations:

$$k_I^q = G\omega\sqrt{d} f_1(x,y) / \left[2\sqrt{2\pi}(1-\nu)\right],$$

$$k_{II}^q = G\omega\sqrt{d} f_2(x,y) / \left[2\sqrt{2\pi}(1-\nu)\right],$$

where

$$f_1(x,y) = \sum_{k=1}^{4} s_k \sqrt{\tilde{r}_k}[3\cos(\theta_k/2) + \cos(3\theta_k/2)],$$
$$f_2(x,y) = \sum_{k=1}^{4} s_k \sqrt{\tilde{r}_k}[\sin(\theta_k/2) + \sin(3\theta_k/2)], \quad (11)$$
$$\tilde{r}_k = r_k/d.$$

Using the above expressions, one can numerically solve Eq. (10) for $K_{IC}$ in the following way. For a preset value of $K_I^\sigma$, one calculates the energy change $\Delta W$ and the equilibrium GB migration lengths $x_0$ and $y_0$ that correspond to a minimum of $\Delta W$. Substituting the obtained values of $x_0$ and $y_0$ into Eq. (11), we deduce the values of $k_I^q$ and $k_{II}^q$. Then we compute the quantities $k_{IC}^q$ and $k_{IIC}^q$ with the assumption that $K_I^\sigma = K_{IC}$. On the next step, we calculate $K_{IC}$ using Eq. (10) and estimate the difference between the so obtained value of $K_{IC}$ and the value of $K_I^\sigma$. Then we vary the preset value of $K_I^\sigma$ and repeat the above procedure until the value of $K_{IC}$ (given by Eq. (10)) becomes equal to the value of $K_I^\sigma$ with sufficient accuracy.

In order to estimate the effect of the disclinations produced by the cooperative GB migration and sliding process (Fig. 1) on crack growth, one should compare the critical stress intensity factor $K_{IC}$ with the quantity $K_{IC}^{br}$. To do so, we have calculated the values of $x_0$ and $y_0$ as well as the ratio $K_{IC}/K_{IC}^{br}$ in the cases of nanocrystalline Ni and nanocrystalline ceramic 3C–SiC with $p = d = 15$ nm, various values of $\omega$ and of the other parameters specified above (for Ni, we also employed $\gamma_b = 0.69$ J m$^{-2}$ [60]; for 3C–SiC, we used [62] $G = 217$ GPa, $\nu = 0.23$, $\gamma = 1.5$ J m$^{-2}$, and $\gamma_b = \gamma/2$). In the case of an intragrain crack in Ni, the calculations give the following results. For $\omega = 45°$, we obtain $x_0/d \approx 0.19$, $y_0/d \approx 0.12$, and $K_{IC}/K_{IC}^{br} \approx 1.78$; for $\omega = 30°$, we obtain $x_0/d \approx 0.47$, $y_0/d \approx 0.34$, and $K_{IC}/K_{IC}^{br} \approx 2.20$; for $\omega = 15°$, we obtain $y_0 = 0$. In this connection, it is noted that at such small enough values of $\omega$, one cannot find the value of $K_{IC}$ using the procedure described above. In other words, in the case under consideration, Eq. (1) for $K_{IC}$ has no solution. The reason is that in this case, an increase in $K_I^\sigma$ increases the equilibrium GB sliding length $x_0$, which allows one to increase $K_I^\sigma$ without inducing crack propagation. An increase in $K_I^\sigma$ leads to further increase in $x_0$ which, in turn, allows to increase $K_I^\sigma$, and so on. For a rough estimate of $K_{IC}/K_{IC}^{br}$ in this case, we assume that the length of GB sliding cannot exceed GB length $d$. Then, for $\omega = 15°$ and $x_0 = d$, we have: $K_{IC}/K_{IC}^{br} \approx 2.53$.

In the case of a GB crack in nanocrystalline Ni, our calculations give the following results. For $\omega = 45°$, we obtain $x_0/d \approx 0.17$, $y_0/d \approx 0.10$, and $K_{IC}/K_{IC}^{br} \approx 1.76$; for $\omega = 30°$, we find $x_0/d \approx 0.40$, $y_0/d \approx 0.27$, and $K_{IC}/K_{IC}^{br} \approx 2.17$; for $\omega = 15°$ and $x_0 = d$, we obtain $K_{IC}/K_{IC}^{br} \approx 2.70$. As is seen, for the same values of $\omega$, the values of the ratio $K_{IC}/K_{IC}^{br}$ characterizing a GB crack are very close to those characterizing an intragrain crack.

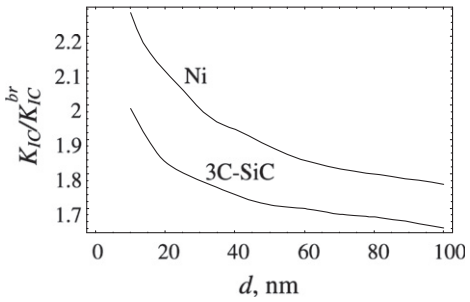


Fig. 5. Normalized critical stress intensity factor $K_{IC}/K_{IC}^{br}$ vs. grain size $d$, in the case of a grain boundary crack in nanocrystalline Ni and 3C–SiC.

Similarly, in the case of an intragrain crack in nanocrystalline ceramic 3C–SiC, one derives the following results. For $\omega = 45°$, we obtain $x_0/d \approx 0.10$, $y_0/d \approx 0.06$, and $K_{IC}/K_{IC}^{br} \approx 1.68$; for $\omega = 30°$, we find $x_0/d \approx 0.21$, $y_0/d \approx 0.13$, and $K_{IC}/K_{IC}^{br} \approx 1.96$; for $\omega = 15°$ and $x_0 = d$, we obtain $K_{IC}/K_{IC}^{br} \approx 3.40$. For a GB crack in 3C–SiC, we have $K_{IC}/K_{IC}^{br} \approx 1.63$, 1.90 and 3.65, for $\omega = 45°$, 30° and 15°, respectively.

Thus, the values of $K_{IC}/K_{IC}^{br}$ in the cases of GB and intragrain cracks are practically the same (at least, for the cases of $\omega = 30°$ and 45°). With these theoretical estimates for nanocrystalline Ni and 3C–SiC, one can conclude that (a) conditions for occurrence of the cooperative GB sliding and migration process near intergrain and intragrain cracks are very similar; (b) the effects of the cooperative GB sliding and migration process on the local stress relaxation near tips of intergrain and intragrain cracks are very similar; and, as a corollary, (c) the effects of the cooperative GB sliding and migration process on crack growth in the cases of intergranular and intragrain fracture processes are very similar.

Now let us consider the effect of grain size on the critical stress intensity factor $K_{IC}$. To do so, we calculated the dependence of $K_{IC}/K_{IC}^{br}$ on grain size $d$ in the case of a GB crack in nanocrystalline Ni and 3C–SiC. The dependences are presented in Fig. 5, for $\omega = 30°$, $p = d$ and other parameter values (typical of nanocrystalline Ni and 3C–SiC) specified above. Fig. 5 demonstrates that, as the grain size increases from 10 to 100 nm, the ratio $K_{IC}/K_{IC}^{br}$ decreases from 2.23 to 1.77, for Ni, and from 1.99 to 1.64, for 3C–SiC. This tendency allows us to conclude that the suggested cooperative GB sliding and migration mechanism is most effective in fracture toughness enhancement in nanocrystalline materials at finest grain sizes. It is contrasted to the situation with lattice dislocation emission from crack tips – the conventional toughening mechanism in metallic materials [63,64] – whose enhancing effect on the fracture toughness of nanocrystalline metals rapidly decreases with a decrease in grain size [65].

In the practically interesting case of nanocrystalline metals at ambient temperatures, one can perform a rough estimate of the cutoff in grain size at which the suggested mechanism of fracture toughness enhancement is essential.

In this case, GB diffusion is too slow to significantly influence the crack growth, and thereby athermal toughening mechanisms dominate. As a consequence, in nanocrystalline metals at ambient temperatures, toughening through the cooperative GB sliding and migration mechanism competes mainly with the conventional toughening mechanism through lattice dislocation emission from crack tips. In order to estimate the discussed cutoff in grain size, we postulate that the cooperative GB sliding and migration mechanism is effective in toughness enhancement, if it increases the critical stress intensity factor larger than lattice dislocation emission from crack tips. In a first approximation, the values of the fracture toughness associated with the two athermal deformation/toughening mechanisms (cooperative GB sliding and migration and lattice dislocation emission from crack tips) are compared using the corresponding normalized critical stress intensity factors. More precisely, we compare the normalized critical stress intensity factor $K_{IC}/K_{IC}^{br}$, which is plotted in Fig. 4 and corresponds to the case shown in Fig. 1, and the factor $\tilde{K}_{IC}/K_{IC}^{br}$ corresponding to the emission of lattice dislocations along one slip plane from a crack tip. The latter factor was calculated in Ref. [65]. The calculations [65] in the cases of Al and α-Fe have demonstrated that, for Al, $\tilde{K}_{IC}/K_{IC}^{br} < 2$ at $d < 40$ nm and $\tilde{K}_{IC}/K_{IC}^{br} > 2$ at $d \geqslant 40$ nm; whereas, for α-Fe, $\tilde{K}_{IC}/K_{IC}^{br} < 2$ at $d < 20$ nm and $\tilde{K}_{IC}/K_{IC}^{br} > 2$ at $d \geqslant 20$ nm. At the same time, in the case shown Fig. 5, $K_{IC}/K_{IC}^{br}$ is ~2, when $d$ is in the range from 20 to 40 nm; and $K_{IC}/K_{IC}^{br} < 2$, when $d > 40$ nm. Therefore, one can conclude that, for nanocrystalline metals at ambient temperatures, the cooperative GB sliding and migration mechanism is effective for fracture toughness enhancement, if the grain size is smaller that the critical grain size being in the range from 20 to 40 nm. Also, note that both lattice dislocation slip and thereby emission of lattice dislocations from crack tips are suppressed in nanocrystalline ceramics at ambient temperatures. In these circumstances, the examined cooperative GB sliding and migration mechanism can play a significant role in increasing fracture toughness of nanocrystalline ceramics at ambient temperatures in a wider range of grain sizes, compared to the situation with metals.

Thus, the results of our calculations show that cooperative GB migration and sliding along a single GB can make the critical stress intensity factor $K_{IC}$ several times larger. Apparently, cooperative GB migration and sliding along various GBs can increase the value of $K_{IC}$ much further and, as a result, may lead to a significant increase of fracture toughness, as compared to the case of pure brittle fracture. For example, if one hypothesizes that cooperative GB migration and sliding can increase the value of $K_{IC}$ by a factor of 5 (as compared to the case of pure brittle intragrain fracture), they would obtain: $K_{IC} = 5K_{IC}^{br} \approx 4.44$ MPa $m^{1/2}$ in the case of nanocrystalline Ni and $K_{IC} \approx 6.50$ MPa $m^{1/2}$ in the case of nanocrystalline 3C–SiC. The latter value of $K_{IC}$ for nanocrystalline 3C–SiC is higher than the typical values (3–4 MPa $m^{1/2}$) of $K_{IC}$ for polycrystalline 3C–SiC at room temperature. At the same time, the obtained value of $K_{IC}$ for nanocrystalline Ni is still much smaller than typical values of $K_{IC}$ for polycrystalline Ni, which are as large as several tens of MPa $m^{1/2}$. However, in combination with other toughening mechanisms (limited dislocation emission from crack tips, stress-driven GB migration, diffusion, etc.), the suggested mechanism of cooperative GB migration and sliding can result in good fracture toughness of nanocrystalline materials, documented in several experiments [29–33].

## 4. Concluding remarks

We have theoretically described the cooperative GB sliding and migration process near crack tips and its effect on the growth of sufficiently large cracks in deformed nanocrystalline metals and ceramics. The cooperative GB sliding and migration deformation mechanism is shown to increase the critical stress intensity factors in nanocrystalline metals and ceramics by several times and, as a result, it may lead to a significant enhancement of fracture toughness of these materials. It is shown that among the two constituents of the examined deformation mechanism (GB sliding and GB migration), GB sliding plays the main role in the enhancement of fracture toughness in nanocrystalline solids. GB migration is essential in the accommodation of GB sliding associated with transfer of high-angle GBs (with a misorientation angle exceeding 21°) (Fig. 1c and d) and, therefore, the enhancing effect of the cooperative GB sliding and migration process on the fracture toughness increases with rising the fraction of high-angle GBs. In the case of GB sliding associated with transfer of low-angle GBs near crack tips, GB sliding can be accommodated through lattice dislocation emission from triple junctions or diffusion [24,28,51].

In general, several deformation mechanisms – lattice dislocation slip, GB sliding, stress-driven GB migration as well as rotational deformation modes and other – can contribute to plastic deformation in nanocrystalline materials (e.g., Refs. [5,17–20,35–37]) and may thus result in fracture toughness enhancement of such materials [39,40,65]. The effect of each mechanism on the fracture toughness of a nanocrystalline specimen depends on the structure of the specimen and its loading conditions. It is the effective combined action of various deformation mechanisms at certain conditions that can provide the experimentally observed [29–33] high fracture toughness of nanocrystalline metals and ceramics.

Finally, note that fracture toughness of nanocrystalline materials can also be analyzed through a mechanism-independent approach based on a theory of nanoelasticity, i.e. linear elasticity enhanced by the Laplasian of strain or stress to account for the higher-order deformation gradients induced by the small volume nanoscale constraints. In particular, enhancement of fracture toughness of nanocrystalline materials may be drawn from the fact [66,67] that the

aforementioned theory of nanoelasticity produces non-singular stress and strain distributions at the crack tip and predicts a maximum stress ahead of it, the value of which depends on the gradient coefficient of nanoscale internal length; therefore, a size-dependent critical stress intensity factor can be determined leading to an enhanced fracture toughness depending on the value of the relevant internal length parameter.

## Acknowledgements

The work was supported, in part, by the Russian Ministry of Education and Science (Contract 14.740.11.0353), and the Russian Academy of Sciences Program "Fundamental studies in nanotechnologies and nanomaterials".

## Appendix A

In the first approximation illustrated in Fig. 2, growth of both intragrain and intergranular (GB) brittle cracks is quantitatively characterized by the critical value of the stress intensity factor $K_{IC}^{br} = \sqrt{4G\gamma_e/(1-\nu)}$. Growth of cracks in grain interiors (Fig. 1a) is specified by the surface energy penalty $\gamma_e = \gamma$ with $\gamma$ being the specific surface energy. In the first approximation (Fig. 2), growth of intergrain cracks (Fig. 2a) is specified by the surface energy penalty $\gamma_e = \gamma - \gamma_b/2$, where $\gamma_b$ is the specific GB energy (released when the crack moves along the GB). In these circumstances, the ratio of the critical stress intensity factor $K_{IC}$ for an intragrain crack to the same factor $K_{IC}$ for a GB crack with the same length is given as follows: $\sqrt{2\gamma/(2\gamma-\gamma_b)}$. The ratio under consideration is approximately equal to 1.12 and 1.19, for nanocrystalline Ni and 3C–SiC, respectively. (In our estimates for nanocrystalline Ni, we used the following typical values of parameters [59,60]: $G = 73$ GPa, $\nu = 0.31$, $\gamma = 1.725$ J m$^{-2}$ and $\gamma_b = 0.69$ J m$^{-2}$. In calculation of the ratio for nanocrystalline 3C–SiC, we used the following typical values of parameters [62]: $G = 217$ GPa, $\nu = 0.23$, $\gamma = 1.5$ J m$^{-2}$ and $\gamma_b = \gamma/2$.) That is, the absolute values of $K_{IC}$ for intragrain cracks in nanocrystalline Ni are ~12% higher than those for GB cracks. In the case of 3C–SiC, the absolute values of $K_{IC}$ for intragrain cracks are ~19% higher than those for GB cracks.

## References

[1] Pande CS, Masumura RA. Mater Sci Eng A 2005;409:125.
[2] Szlufarska I, Nakano A, Vashista P. Science 2005;309:911.
[3] Barai P, Weng GJ. Acta Mech 2008;195:327.
[4] Barai P, Weng GJ. Int J Plast 2008;24:1380.
[5] Wei Y, Bower AF, Gao H. Acta Mater 2008;56:1741.
[6] Weng GJ. Rev Adv Mater Sci 2009;19:41.
[7] Yang F, Yang W. J Mech Phys Solids 2009;57:305–24.
[8] Rösner H, Boucharat N, Padmanabhan KA, Markmann J, Wilde G. Acta Mater 2010;58:2610.
[9] Gerlich AP, Yue L, Mendez PF, Zhang H. Acta Mater 2010;58:2176.
[10] Swaminathan N, Kamenski PJ, Morgan D, Szlufarska I. Acta Mater 2010;58:2843.
[11] Danaie M, Tao SX, Kalisvaart P, Mitlin D. Acta Mater 2010;58:3162.
[12] Jonnalagadda K, Karanjgaokar N, Chasiotis I, Chee J, Peroulis D. Acta Mater 2010;58:4674.
[13] Huang P, Wang F, Xu M, Xu KW, Lu TJ. Acta Mater 2010;58:5196.
[14] Bachurin DV, Gumbsch P. Acta Mater 2010;58:5491.
[15] Kim D-H, Manuel MV, Ebrahimi F, Tulenko JS, Phillpot SR. Acta Mater 2010;58:6217.
[16] Kuntz JD, Zhan G-D, Mukherjee AK. MRS Bull 2004;29:22.
[17] Ovid'ko IA. Int Mater Rev 2005;50:65.
[18] Wolf D, Yamakov V, Phillpot SR, Mukherjee AK, Gleiter H. Acta Mater 2005;53:1.
[19] Dao M, Lu L, Asaro RJ, De Hosson JTM, Ma E. Acta Mater 2007;55:4041.
[20] Mukhopadhyay A, Basu B. Int Mater Rev 2007;52:257.
[21] Aifantis EC. Mater Sci Eng A 2009;503:190.
[22] Pande CS, Cooper KP. Prog Mater Sci 2009;54:689.
[23] Padilla II HA, Boyce BL. Exp Mech 2001;50:5.
[24] Koch CC, Ovid'ko IA, Seal S, Veprek S. Structural nanocrystalline materials: fundamentals and applications. Cambridge: Cambridge University Press; 2007.
[25] Cheng S, Ma E, Wang YM, Kecskes LJ, Youssef KM, Koch CC, et al. Acta Mater 2005;53:1521.
[26] Youssef KM, Scattergood RO, Murty KL, Horton JA, Koch CC. Appl Phys Lett 2005;87:091904.
[27] Youssef K-M, Scattergood RO, Murty KL, Koch CC. Scripta Mater 2006;54:251.
[28] Sergueeva AV, Mara NA, Mukherjee AK. J Mater Sci 2007;42:1433.
[29] Bhaduri S, Bhaduri SB. Nanostruct Mater 1997;8:755.
[30] Mirshams RA, Liao CH, Wang SH, Yin WM. Mater Sci Eng A 2001;315:21.
[31] Zhao Y, Qian J, Daemen LL, Pantea C, Zhang J, Voronin GA, et al. Appl Phys Lett 2004;84:1356.
[32] Kaminskii AA, Akchurin MS, Gainutdinov RV, Takaichi K, Shirakava A, Yagi H, et al. Crystallogr Rep 2005;50:869.
[33] Pei YT, Galvan D, De Hosson JTM. Acta Mater 2005;53:4505.
[34] Masumura RA, Hazzledine PM, Pande CS. Acta Mater 1998;46:4527.
[35] Milligan WW, Hackney SA, Aifantis EC. Nanostruct Mater 1993;2:267.
[36] Ke M, Hackney SA, Milligan WW, Aifantis EC. Nanostruct Mater 1995;5:689.
[37] Aifantis EC. In: Katsikadelis T, Beskos DE, Gdonfos EE, editors. Recent advances in applied mechanics (honorary volume for Academician A.N. Kounadis). Athens: NTU; 2000. p. 243–54.
[38] Gutkin MY, Mikaelyan KN, Ovid'ko IA. Scripta Mater 2008;58:850.
[39] Morozov NF, Ovid'ko IA, Sheinerman AG, Aifantis EC. J Mech Phys Solids 2010;58:1088.
[40] Ovid'ko IA, Sheinerman AG, Aifantis EC. Acta Mater 2008;56:2718.
[41] Jin M, Minor AM, Stach EA, Morris Jr JW. Acta Mater 2004;52:5381.
[42] Soer WA, De Hosson JTM, Minor AM, Morris Jr JW, Stach EA. Acta Mater 2004;52:5783.
[43] Gutkin MY, Ovid'ko IA. Appl Phys Lett 2005;87:251916.
[44] Sansoz F, Dupont V. Appl Phys Lett 2006;89:111901.
[45] Dupont V, Sansoz F. Acta Mater 2008;56:6013.
[46] Rupert TJ, Gianola DS, Gan Y, Hemker KJ. Science 2009;326:1686.
[47] Gianola DS, Van Petegem S, Legros M, Brandstetter S, Van Swygenhoven H, Hemker KJ. Acta Mater 2006;54:2253.
[48] Cheng S, Zhao Y, Wang Y, Li Y, Wang X-L, Liaw PK, et al. Phys Rev Lett 2010;104:255501.
[49] Ovid'ko IA, Sheinerman AG. Appl Phys Lett 2007;90:171927.
[50] Ovid'ko IA, Sheinerman AG. Acta Mater 2009;57:2217.
[51] Sergueeva AV, Mara NA, Krasilnikov NA, Valiev RZ, Mukherjee AK. Philos Mag 2006;86:5797.
[52] Bobylev SV, Morozov NF, Ovid'ko IA. Phys Rev Lett 2010;105:055504.
[53] Mukherjee AK. Mater Sci Eng A 2002;322:1.
[54] Li H, Ebrahimi F. Appl Phys Lett 2004;84:4307.
[55] Li H, Ebrahimi F. Adv Mater 2005;17:1969.

[56] Ebrahimi F, Liscano AJ, Kong D, Zhai Q, Li H. Rev Adv Mater Sci 2006;13:33.
[57] Romanov AE, Vladimirov VI. In: Nabarro FRN, editor. Dislocations in solids, vol. 9. Amsterdam: North-Holland; 1992. p. 191–302.
[58] Panasyuk VV, editor. Fracture mechanics and strength of materials, vol. 2. Kiev: Naukova Dumka; 1988 [in Russian].
[59] Smithells CJ, Brands EA. Metals reference book. London: Butterworth; 1976.
[60] Hirth JP, Lothe J. Theory of dislocations. New York: Wiley; 1982.
[61] Irwin RG. J Appl Mech 1957;24:361.
[62] Ding Z, Zhou S, Zhao Y. Phys Rev B 2004;70:184117.
[63] Rice JR, Thompson RM. Philos Mag 1974;29:73.
[64] Rice JR. J Mech Phys Solids 1992;40:239.
[65] Ovid'ko IA, Sheinerman AG. Acta Mater 2010;58:5286.
[66] Aifantis EC. Microsyst Technol 2009;15:109.
[67] Aifantis EC. Int J Eng Sci 2009;47:1089.